ELSEVIER

Contents lists available at ScienceDirect

Solid State Communications

journal homepage: www.elsevier.com/locate/ssc



Full length article

Heat currents in a two channel Marcus molecular junction

Natalya A. Zimbovskaya

Department of Physics and Electronics, University of Puerto Rico-Humacao, CUH Station, Humacao, PR 00791, USA

ARTICLE INFO

Communicated by Josep Fontcuberta

Keywords:
Electron transport through molecular junctions
Marcus theory
Heat currents

ABSTRACT

We present a theoretical analysis of heat transfer in a single-molecule junction where the bridge is simulated by a three-state model with two possible transport channels for electrons. Interactions between electrons on the bridge and phonons in the nuclear environment are supposed to be strong, so that Marcus-type processes predominate in the electron transport. It is shown that asymmetric coupling between the bridge states and electrodes and/or asymmetric distribution of the bias voltage over the system together with characteristics of the environmental reorganization and relaxation processes accompanying electron transport may result in qualitative changes in the behavior of steady state heat currents. These changes are controlled by the same mechanism as NDR effect manifested in the charge current under similar conditions. Also, we analyze the energy balance in single-molecule junctions assuming that energy levels of the molecule are slowly driven by an external force.

1. Introduction

Presently, molecular electronics [1–5] is a fast developing field providing a general platform to realize diverse atomic-scale devices. The basing building block for such devices is a single molecule junction (SMJ) that is a molecule linking two conducting (metallic/semiconductor) electrodes. Electron transfer through SMJs may be driven by electric forces and thermal gradients. In general, one may separate out two extreme limits for the electron transport through a SMJ. Within one limit the transport is nearly ballistic, and electron interactions with vibrational modes associated with the molecule as well as with thermalized phonons associated with its ambient may be treated as perturbations [6–8].

Within another limit, electron transport is strongly affected by thermal phonons associated with random nuclear motions in the molecule's environment. Within this limit, electron transfer in the SMJ may be viewed as a sequence of hops between the electrodes and the states on the molecular linker where the traveling electron may be transiently localized by distorting its close ambient. In some cases SMJs operate being immersed in a dielectric solvent, and the solvent response may cause significant changes in transport characteristics [9–11]. In the present work we focus on such 'wet' systems. However, the obtained results may be easily generalized to include 'dry' SMJs which do not feature liquid environments.

In the regime of strong electron–phonon interaction electron transport along molecules may be analyzed by using Marcus theory [12–14] or its extensions [15–20]. These theories were repeatedly and successfully employed to study charge transport through molecules [21–27].

In particular, it was shown that influence of the molecular environment may result in such interesting effects as charge current rectification and NDR [23,24,27–30]. Specifically, NDR may appear in a multichannel system as a result of competition between the transport channels [27, 31].

Heat transfer in Marcus junctions was also studied [15,16,32]. Nevertheless, the analysis of heat conduction through Marcus SMJs is not completed so far. In the present work we contribute to this subject matter by analyzing the effect of competition between transport channels on heat transfer processes accompanying electron transport in such systems. Note that there also exists purely phonon heat transfer which was extensively studied in the last two decades (see e.g [33,34]). However, phonon currents may occur provided that the electrodes are kept at different temperatures. In the present work we assume that the temperature remains the same over the system thus preventing the emergence of phonon currents. In Section 2 we consider steady state heat currents through a SMJ with two transport channels within Marcus transport regime and show that electron heat currents may decrease when the bias voltage strengthens. In Section 3, we analyze the energy balance in the considered system assuming that the bridge levels are slowly driven by an external force. Conclusions are presented in Section 4.

2. Steady state heat currents in a two channel system

As a model for the two channel bridge linking the electrodes in a SMJ we choose a molecule with three states $|a\rangle$, $|b\rangle$ and $|c\rangle$

E-mail address: natalya.zimbovskaya@upr.edu.

accessible within the considered range of the bias voltage V. We assume that the states |a> and |c> are different charged states of the molecule, and the molecule is neutral being in the state |b>. Also, we assume that only a single electron may be injected/removed to/from the states |a> and |c>. States corresponding to a doubly charged molecule are supposed to be inaccessible within the bias voltage range. The model considered here includes strong coupling to the phonon environment at the cost of treating this coupling semiclassically and assuming weak coupling between molecule and electrodes.

Probabilities P_a , P_b and P_c for the molecule to be in these states at a certain moment t ($P_a + P_b + P_c = 1$) are given by kinetic equations [27,31]:

$$\frac{dP_a}{dt} = P_b \cdot k_{ba} - P_a \cdot k_{ab} \tag{1}$$

$$\frac{dP_b}{dt} = P_a \cdot k_{ab} + P_c \cdot k_{cb} - P_b \cdot \left(k_{ba} + k_{bc}\right) \tag{2}$$

$$\frac{dP_c}{dt} = P_b \cdot k_{bc} - P_c \cdot k_{cb} \tag{3}$$

Here, $k_{ab}=k_{ab}^L+k_{ab}^R$, $\alpha=\{a,c\}$ and Marcus approximations for the transfer rates are given by [12,13]:

$$k_{\alpha b}^{K} = \sqrt{\frac{\beta_{s}}{4\pi\lambda_{\alpha}}} \Gamma_{\alpha}^{K} \int_{-\infty}^{\infty} d\epsilon [1 - f_{K}(\beta_{K}, \epsilon)] \times \exp\left[-\frac{\beta_{s}}{4\lambda_{\alpha}} (\epsilon + \lambda_{\alpha} - \epsilon_{\alpha})^{2}\right], \tag{4}$$

$$k_{b\alpha}^{K} = \sqrt{\frac{\beta_{s}}{4\pi\lambda_{\alpha}}} \Gamma_{\alpha}^{K} \int_{-\infty}^{\infty} d\epsilon f_{K}(\beta_{K}, \epsilon) \times \exp\left[-\frac{\beta_{s}}{4\lambda_{\alpha}} (\epsilon_{\alpha} + \lambda_{\alpha} - \epsilon)^{2}\right], \tag{5}$$

Here, $K=\{L,R\}$, $\epsilon_{\alpha}=E_{\alpha}-E_{b}$ (E_{α},E_{b} being the energies associated with molecular states $|\alpha>$ and |b>), λ_{α} are reorganization energies corresponding to $|\alpha>\to|b>$ and $|b>\to|\alpha>$ transitions, Γ_{α}^{K} are bare electron transfer rates between the molecular state $|\alpha>$ and the left/right electrode, $\beta_{K}=\frac{1}{kT_{K}}$ and $\beta_{s}=\frac{1}{kT_{s}}$ indicate the temperatures of the electrodes and that of the solvent, k is the Boltzmann constant and $f_{K}(\beta_{K},\epsilon)$ are Fermi distribution functions for the electrodes with chemical potentials μ_{K} . Strictly speaking, the transfer rates Γ_{α}^{K} depend on energy but we disregard these dependencies using the wide band approximation for electrodes.

As follows from these expressions, transfer rates k_{ab}^K and k_{ba}^K respectively refer to the electron transfer from the charged molecule to an electrode K thus bringing the molecule to the neutral state |b> and to the injection of an electron to the neutral molecule. In further analysis we assume that $T_L = T_R = T_s$. Steady state probabilities P_a^0 , P_b^0 and P_c^0 may be computed from Eqs. (1)–(3):

$$P_b^0 = \frac{1}{1 + \frac{k_{ba}}{k_{c}} + \frac{k_{bc}}{k_{c}}}; \qquad P_a^0 = P_b^0 \frac{k_{ba}}{k_{ab}}; \qquad P_c^0 = P_b^0 \frac{k_{bc}}{k_{cb}}.$$
 (6)

The results for the probabilities computed assuming that the bias voltage is symmetrically distributed over the system ($\mu_{L,R} = \mu \pm \frac{\mathrm{eV}}{2}$ where the chemical potential μ corresponds to an unbiased system) and $\epsilon_c > \epsilon_a$ are presented in Fig. 1. As shown in this figure, the charged states |a> and |c> become occupied either successively or simultaneously indicating successive/simultaneous opening of the corresponding transport channels. The order of succession is controlled by the relationship between the state energies ϵ_a and the reorganization energies λ_a . The latter take an important part in determining the succession order. It may happen that the channel associated with the higher energy ϵ_c opens up at lower bias than that associated with the lower energy ϵ_a provided that λ_a significantly exceeds λ_c , as shown in the lower panel of Fig. 1.

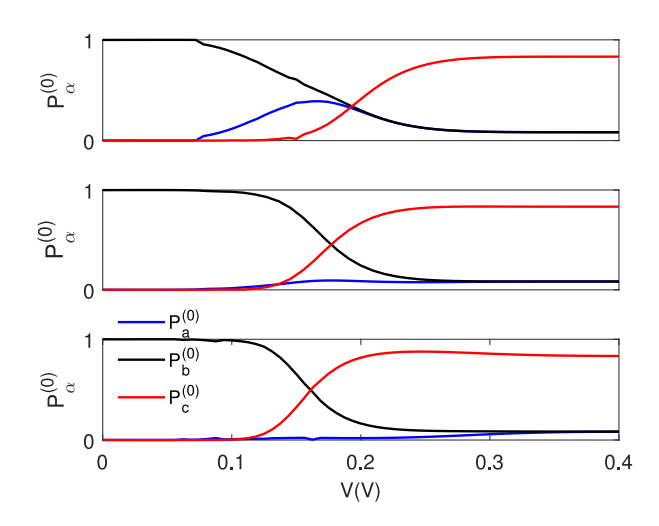


Fig. 1. Steady state probabilities plotted for a two channel Marcus SMJ as functions of the bias voltage assuming that $T_L = T_R = T_s = 2.6$ meV, $\Gamma_a^L = \Gamma_a^R = \Gamma_c^L = 5$ meV, $\Gamma_c^R = 0.1\Gamma_c^L$, $\epsilon_a = 0.02$ eV, $\epsilon_c = 0.06$ eV and $\lambda_a = 0.05$ eV, $\lambda_c = 0.06$ eV (top panel); $\lambda_a = 0.09$ eV, $\lambda_c = 0.05$ eV (middle panel); $\lambda_a = 0.12$ eV, $\lambda_c = 0.04$ eV (bottom panel).

The steady state charge current I_{ss} is given by the expression:

$$\frac{I_{ss}}{\rho} = k_{ba}^{L} P_{b}^{0} + k_{bc}^{L} P_{b}^{0} - k_{ab}^{L} P_{a}^{0} - k_{cb}^{L} P_{c}^{0}$$

$$\tag{7}$$

which could be reduced to the form [27]:

$$\frac{I_{ss}}{e} = \frac{\left(I_1 \left(1 + \frac{k_{ba}}{k_{ab}}\right) + I_2 \left(1 + \frac{k_{bc}}{k_{cb}}\right)\right)}{\left(1 + \frac{k_{ba}}{k_{ab}} + \frac{k_{bc}}{k_{cb}}\right)}$$
(8)

where

$$I_{1} = \frac{k_{ab}^{R} k_{ba}^{L} - k_{ab}^{L} k_{ba}^{R}}{k_{ab} + k_{ba}}; \qquad I_{2} = \frac{k_{cb}^{R} k_{bc}^{L} - k_{cb}^{L} k_{bc}^{R}}{k_{cb} + k_{bc}}$$
(9)

Note that eI_1 represents the charge current flowing through the system provided that transitions $|b>\leftrightarrow|c>$ are inaccessible, and eI_2 takes on the similar part in the case of inaccessibility of transitions $|b>\leftrightarrow|a>$. In the expression for I_{ss} each of these currents is multiplied by the probability showing that the corresponding transport channel is active.

Each electron hop between the molecule and an electrode is accompanied by heat production in both electrodes and solvent environment of the molecule originating from their relaxation. We denote the heat produced in the solvent as Q_s and that produced in the electrodes as Q_e . Specifically, $Q_{s,ab}^K$ and $Q_{s,ba}^{K}$ are heat changes in the solvent when an electron hops to (from) K electrode from (to) the molecule state $|\alpha>$. Within Marcus approach these heats may be written in the form similar to that used in earlier works [16]:

$$Q_{s,ab}^{K} = \frac{\Gamma_{\alpha}^{K}}{k_{ab}^{K}} \sqrt{\frac{\beta_{s}}{4\pi\lambda_{\alpha}}} \int_{-\infty}^{\infty} d\epsilon \left[1 - f_{K}(\beta_{K}, \epsilon)\right] (\epsilon_{\alpha} - \epsilon)$$

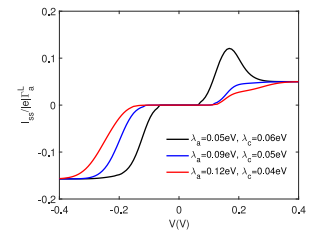
$$\times \exp\left[-\frac{\beta_{s}}{4\lambda_{\alpha}} (\lambda_{\alpha} - \epsilon_{\alpha} + \epsilon)^{2}\right].$$
(10)

and

$$Q_{s,b\alpha}^{K} = \frac{\Gamma_{\alpha}^{K}}{k_{b\alpha}^{K}} \sqrt{\frac{\beta_{s}}{4\pi\lambda_{\alpha}}} \int_{-\infty}^{\infty} d\epsilon f_{K}(\beta_{K}, \epsilon)(\epsilon - \epsilon_{\alpha}) \times \exp\left[-\frac{\beta_{s}}{4\lambda_{\alpha}}(\epsilon_{\alpha} + \lambda_{\alpha} - \epsilon)^{2}\right]. \tag{11}$$

Heats $Q_{e,ab}^K$ and $Q_{e,ba}^K$ generated in the electrode K when an electron leaves (enters) $|\alpha\rangle$ state on the molecule and arrives to (leaves from) this electrode may be approximated by the following expressions:

$$Q_{e,\alpha b}^{K} = \frac{\Gamma_{\alpha}^{K}}{k_{\alpha b}^{K}} \sqrt{\frac{\beta_{s}}{4\pi \lambda_{\alpha}}} \int_{-\infty}^{\infty} d\epsilon \left[1 - f_{K}(\beta_{K}, \epsilon)\right] (\epsilon - \mu_{K})$$



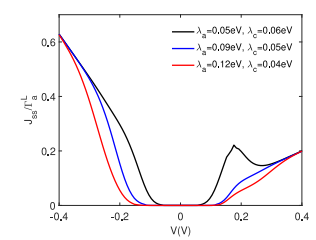


Fig. 2. The steady state charge current I_{ss} (left panel) and the sum of heat currents J_{ss} (right panel) plotted as functions of the bias voltage at $T_L = T_R = T_s = 2.6$ meV, $\Gamma_a^L = \Gamma_a^R = \Gamma_c^L = 10\Gamma_c^R$, $\Gamma_a^L = 5$ meV, $\epsilon_a = 0.02$ eV, $\epsilon_c = 0.06$ eV for several values of the reorganization energies.

$$\times \exp\left[-\frac{\beta_s}{4\lambda_\alpha}(\lambda_\alpha - \epsilon_\alpha + \epsilon)^2\right]. \tag{12}$$

and

$$Q_{e,b\alpha}^{K} = \frac{\Gamma_{\alpha}^{K}}{k_{b\alpha}^{K}} \sqrt{\frac{\beta_{s}}{4\pi\lambda_{\alpha}}} \int_{-\infty}^{\infty} d\epsilon f_{K}(\beta_{K}, \epsilon)(\mu_{K} - \epsilon)$$

$$\times \exp\left[-\frac{\beta_{s}}{4\lambda_{\alpha}}(\epsilon_{\alpha} + \lambda_{\alpha} - \epsilon)^{2}\right]. \tag{13}$$

In the following analysis integrals in Eqs. (10)–(13) as well as those in the expressions for the transfer rates Eq. (4), (5) are computed numerically for the corresponding analytical expressions are too cumbersome to be useful.

The corresponding heat change rates (heat currents associated with the electron transport) in the solvent $(J_s = \dot{Q}_s)$ and electrodes $(J_e^K = \dot{Q}^K)$ are:

$$J_{s} = P_{a}^{0}(k_{ab}^{L}Q_{s,ab}^{L} + k_{ab}^{R}Q_{s,ab}^{R}) + P_{c}^{0}(k_{cb}^{L}Q_{s,cb}^{L} + k_{cb}^{R}Q_{s,cb}^{R})$$

$$+ P_{b}^{0}(k_{ba}^{L}Q_{s,ba}^{L} + k_{ba}^{R}Q_{s,ba}^{R} + k_{bc}^{L}Q_{s,bc}^{L} + k_{bc}^{R}Q_{s,bc}^{R})$$

$$(14)$$

and

$$J_{e}^{K} = P_{a}^{0} k_{ab}^{K} Q_{e,ab}^{K} + P_{b}^{0} k_{ba}^{K} Q_{e,ba}^{K}$$

$$+ P_{c}^{0} k_{cb}^{K} Q_{e,cb}^{K} + P_{b}^{0} k_{bc}^{K} Q_{e,bc}^{K}$$

$$(15)$$

Summing up all heat currents and using Eqs. (4),(5) as well as Eqs. (10)–(13) we may show that Eqs. (14) and (15) imply that:

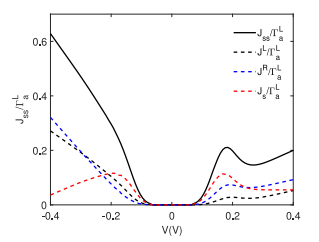
$$J_{ss} = J_e^L + J_e^R + J_s = (\mu_L - \mu_R) \frac{I_{ss}}{2}$$
 (16)

thus conforming the balance between the power given to the system by applying the bias voltage ($\mu_L - \mu_R = \text{eV}$) and the heat currents deposited into the electrodes and the solvent.

Dependencies of both I_{ss} and J_{ss} on the bias voltage are shown in Fig. 2. All functions plotted in this figure take on nonzero values only when a sufficiently strong bias is reached. This happens because at weaker bias the system is unable to overcome the Franck–Condon blockade [35,36] originating from electrons interactions with solvent phonons. Also, all plotted curves show asymmetry with respect to the voltage polarity which originates from asymmetric coupling of one of the transport channels to the electrodes.

We may analyze charge and heat currents behavior at the bias voltage polarity corresponding to $\mu_L > \mu_R$ and chosen values of the energies basing on the expressions given by Eqs. (14),(15). It follows that at low bias and close values of the reorganization energies the ratio $\frac{k_{bc}}{k_{cb}}$ is much smaller than the ratio $\frac{k_{ba}}{k_{ab}}$, so the charge current is determined by the contribution I_1 . At higher voltage, the transport channel associated with the state |c> becomes accessible. However, the increase of V is accompanied with the enhancement of the ratio $\frac{k_{bc}}{k^R}$

approaching the value of $\frac{\Gamma_c^L}{\Gamma_c^R}$ which is significantly greater than unity. Accordingly, the state |c> becomes a blocking state where the traveling electron could be temporarily trapped. This leads to the decrease of



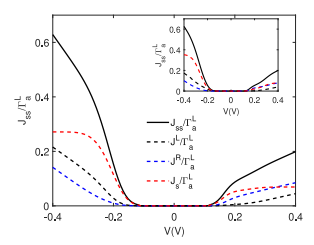
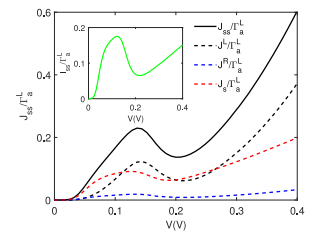


Fig. 3. Steady state heat currents J_s , J_e^L and J_e^R as functions of the bias voltage plotted at $T_L = T_R = T_s = 2.6$ meV, $\Gamma_a^L = \Gamma_a^R = \Gamma_c^L = 10\Gamma_c^R$, $\Gamma_a^L = 5$ meV, $\epsilon_a = 0.02$ eV, $\epsilon_c = 0.06$ eV, $\mu_{L,R} = \pm \frac{\rm eV}{2}$. Left panel: $\lambda_a = 0.05$ eV, $\lambda_c = 0.06$ eV. Right panel: $\lambda_a = 0.12$ eV, $\lambda_c = 0.04$ eV (main body) and $\lambda_a = 0.09$ eV, $\lambda_c = 0.05$ eV (inset).



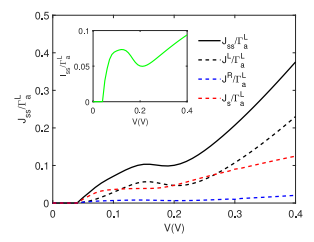


Fig. 4. Steady state heat currents J_s , J_e^L and J_e^R as functions of the bias voltage plotted at $T_L = T_R = T_s = 2.6$ meV, $\epsilon_a = 0.02$ eV, $\epsilon_c = 0.06$ eV, $\lambda_a = 0.03$ eV, $\lambda_c = 0.12$ eV $\eta = 0.9$. Left panel: $\Gamma_a^L = \Gamma_a^R = \Gamma_c^L = \Gamma_c^R = 5$ meV. Right panel: $\Gamma_a^L = \Gamma_c^L = 1$ meV; $\Gamma_a^R = \Gamma_c^R = 5$ meV. Insets show NDR in the corresponding charge currents behavior.

the charge current manifested as NDR. At further strengthening of the bias the charge current levels off at the value controlled by competition between two active transport channels [27]. The NDR effect in current–voltage curves displayed in the left panel of Fig. 2.

The same mechanism is responsible for the appearance of a similar feature in J_{ss} versus V curve under the same conditions, as illustrated in the right panel of this figure. These features disappear when both |a> and |c> become occupied at the same voltage, and the transport channels simultaneously open up. Finally, it may happen that the reorganization energy λ_a significantly exceeds λ_c and the channel associated with the higher energy ϵ_c becomes active at lower bias voltage, as illustrated in the bottom panel of Fig. 1. However, the inverted order of accessibility of the transport channels does not bring back NDR or similar effects in the heat currents behavior.

Steady state heat currents J_s , J_e^L and J_e^R are separately displayed in Fig. 3. One may conclude that the mechanism giving rise to NDR leads to the negative differential heat conductance (NDHC) appearing in the heat current to the solvent J_s . Similar, although less distinct features may be observed in the behavior of heat currents J_{ρ}^{K} flowing to the electrodes. This is shown in the left panel of the figure. As the difference between λ_a and λ_c ($\lambda_a > \lambda_c$) increases, the two transport channels become accessible nearly simultaneously, and the NDHC effect is fading away along with the NDR. This is illustrated in the right panel of Fig. 3. Note that in this case, as well as in the case when the order of succession of transport channels is inverted, the heat current J_{ϵ} shows more pronounced asymmetry with respect to the voltage polarity than currents J_a^K . When $\mu_L < \mu_R$, the heat current flowing to the solvent significantly exceeds currents flowing to the electrodes, whereas in the case of the reversed bias ($\mu_L > \mu_R$) all heat currents are close in magnitude. Comparing profiles of the curves plotted in the main body of right panel of the Fig. 3 with those displayed in the inset we may conclude that when the blocking of |c> to |b> transitions disappears, the difference in the values of reorganization energies λ_{α} does not bring qualitative changes into the heat currents behavior.

As already shown in earlier works, NDR may appear in the situation when both states on the molecular bridge are symmetrically and equally coupled to the electrodes ($\Gamma_a^L = \Gamma_a^R = \Gamma_c^L = \Gamma_c^R$) provided that

the bias is asymmetrically distributed over the system ($\mu_L = \mu + \eta eV$, $\mu_R = \mu - (1 - \eta) \text{eV}$), and this asymmetry is sufficiently pronounced. In the case when $\eta \sim 1$ (that is the bias voltage mostly shifts the chemical potential of the left electrode) and the reorganization energy λ_c significantly exceeds ϵ_c preventing |c> to |b> transitions on the right electrode. Then a single transport channel associated with ϵ_a is open at low bias voltage. As the voltage increases, it first results in high probability for the transferring electron to be trapped at $|c\rangle$ state thus bringing the NDR [27]. At further increase of V both transport channels become effective, and current enhances again. The same mechanism controls the behavior of heat currents presented in Fig. 4. The assumed asymmetry in the bias voltage distribution leads to the reduced heat transfer to the right electrode of both J_s and J_L . The latter heat currents show NDHC effect, as well as the total heat current J_{ss} . Note that this effect is more distinct when the bridge is symmetrically coupled to the electrodes, as follows from comparison of the curves plotted in the left and right panels of this figure.

3. Heat currents and work in a driven junction

Now, we turn to the analysis of energy currents in a driven two channel junction. The driving is modeled by time dependence of the molecule states energies. The driving may be achieved by varying the corresponding gate potential. Transport properties of driven junctions with negligible electron–phonon interactions and a single transport channel were studied in several works [37–40]. On the contrary, the model adopted here postulates strong coupling to the phonon environment. Similar model was used to study heat currents and work done in a driven junction with a single transport channel [32].

We assume that the energies ϵ_a are varying slowly, that is $\dot{\epsilon}_a$ and $\dot{\epsilon}_c$ are small compared to $kT_s\Gamma_a^K$ and $\frac{(\Gamma_a^K)^2}{h}$. Then we present the population probabilities as sums of their steady state values and time dependent corrections:

$$P_{a}(t) = P_{a}^{0}(\epsilon_{a}) - G_{a}(t); \qquad P_{c}(t) = P_{c}^{0}(\epsilon_{c}) - G_{c}(t);$$
 (17)

and $G_b = -(G_a + G_c)$. Here, we restrict our consideration by first order corrections linear in \dot{e}_α and \dot{e}_α which is justified for the case of quasistatic processes. Then using Eqs. (1)–(3) we get the following approximations:

$$G_a = \frac{\dot{\epsilon}_a (k_{cb} + k_{bc}) \frac{\partial P_a^0}{\partial \epsilon_a} - \dot{\epsilon}_c k_{ba} \frac{\partial P_c^0}{\partial \epsilon_c}}{(k_{ab} + k_{ba})(k_{cb} + k_{bc}) - k_{bc} k_{ba}}; \tag{18}$$

$$G_c = \frac{\dot{\epsilon}_c (k_{ab} + k_{ba}) \frac{\partial P_c^0}{\partial \epsilon_c} - \dot{\epsilon}_a k_{bc} \frac{\partial P_a^0}{\partial \epsilon_a}}{(k_{ab} + k_{ba})(k_{cb} + k_{bc}) - k_{bc} k_{ba}};$$
(19)

Electronic currents now differ from their steady state values and acquire corrections $I_{\nu}^{(1)}$:

$$I_{L}^{(1)} = G_a \left(k_{ba}^L + k_{ab}^L \right) + G_c \left(k_{bc}^L + k_{cb}^L \right) \tag{20}$$

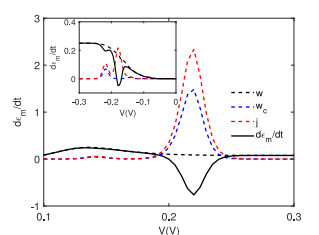
$$I_{p}^{(1)} = G_{q} \left(k_{bq}^{R} + k_{qb}^{R} \right) + G_{c} \left(k_{bc}^{R} + k_{qb}^{R} \right) \tag{21}$$

Similarly, corrections proportional $\dot{\epsilon}_{\alpha}$ appear in the expressions for heat currents. Introducing the total heat current $J=J_e^L+J_e^R+J_s$ we may present it in the form $J=J_{ss}+J^{(1)}$ where J_{ss} is the steady state heat current which is equal to the sum of currents given by Eqs. (14) and (15). The correction $J^{(1)}$ equals:

$$J^{(1)} = \mu_L \left(I_L^{(1)} + G_a k_{bc}^L + G_c k_{ba}^L \right) + \mu_R \left(I_R^{(1)} + G_a k_{bc}^R + G_c k_{ba}^R \right)$$

$$- G_a \left(\epsilon_a (k_{ab} + k_{ba}) + \epsilon_c k_{cb} \right) - G_c \left(\epsilon_a k_{ab} + \epsilon_c (k_{cb} + k_{bc}) \right)$$
(22)

To better elucidate the meaning of this result we consider a simplified case assuming that driving of each molecule's level does not disturb



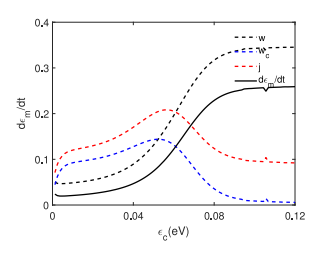


Fig. 5. Illustration of the molecular energy conservation in a driven junction given by Eq. (24). The displayed curves represent dependencies of the reduced reversible power $w=\frac{W}{\epsilon}$ and the reduced rates of chemical work $w_c=\frac{W_{chm}}{\epsilon}$ and of the electron heat current $j=\frac{J}{\epsilon}$ on the bias voltage (left) and on the energy ϵ_c at a fixed value of the bias voltage. The curves are plotted assuming that $\dot{\epsilon}_a=\dot{\epsilon}_c$, $T_L=T_R=T_s=2.6$ meV, $\Gamma_a^L=\Gamma_a^R=\Gamma_c^L=10\Gamma_c^R$, $\Gamma_a^L=5$ meV, $\epsilon_a=0.02$ eV, $\lambda_a=0.1$ eV, $\lambda_c=0.05$ eV, $\epsilon_c=0.04$ eV, (left panel) and V=0.2 V (right panel).

electron transfer processes between electrodes and another level. Then Eq. (22) may be reduced to the form:

$$J^{(1)} = \mu_L I_L^{(1)} + \mu_R I_R^{(1)} - \epsilon_a \dot{\epsilon}_a \frac{\partial P_a^0}{\partial \epsilon} - \epsilon_c \dot{\epsilon}_c \frac{\partial P_c^0}{\partial \epsilon}$$
 (23)

Rearranging the last two terms we get:

$$\frac{d}{dt} \left(\epsilon_a P_a^{(0)} + \epsilon_c P_c^{(0)} \right) = \dot{\epsilon}_a P_a^{(0)} + \dot{\epsilon}_c P_c^{(0)} + \mu_L I_L^{(1)} + \mu_R I_R^{(1)} - J^{(1)}$$
 (24)

which is an analog of the corresponding result derived for a single channel junction [32]. This expression confirms the first law of thermodynamics written for a quasistatic process. On the left side we have the rate of change of the molecular energy \dot{E}_m caused by the driving of the molecular levels. It is equal to the sum of the reversible power $W=\dot{\epsilon}_a P_a^{(0)}+\dot{\epsilon}_c P_c^{(0)}$, the rate of chemical work $W_{chem}=\mu_L I_L^{(1)}+\mu_R I_R^{(1)}$ and the heat current coming from the environment $-J^{(1)}$.

We separately plot these terms as functions of the bias voltage in the left panel of Fig. 5 assuming that $\dot{\epsilon}_c = \dot{\epsilon}_a = \dot{\epsilon}$ As shown in this figure, \dot{E}_m practically coincides with the power term everywhere, except vicinities of the points $\lambda_a = \frac{1}{2}V \pm \epsilon_a$ which indicate the opening and closing of transport channels as they cross boundaries of the conduction window determined by the bias voltage. Near these points both heat currents and chemical work strongly contribute to \dot{E}_m but their contributions counterbalance each other to a significant extent, so the total effect remains rather moderate. Specifically, in Fig. 5 we see the described features at $\epsilon_a + \lambda_a = \frac{1}{2}$ V (main body) and $\epsilon_a - \lambda_a = \frac{1}{2}$ V (inset).

To further elucidate the effect of the higher level transport channel on transport properties of a two channel system we study the behavior of w, w_c and j as functions of the energy ε_c at fixed ε_a , λ_a , λ_c and V. The results are displayed in the right panel of Fig. 5. At small values of ε_c all contributions to \dot{E}_M rather weakly depend on the latter. However, when ε_c approaches the value corresponding to the opening up the channel associated with the state |a> magnitudes of all contributions to \dot{E}_M show rapid changes. At further increase of ε_c they level off again.

4. Conclusions

In the present work we have studied heat currents associated with electron transfer in single molecule junctions where the bridge was modeled by a three-state molecule connecting free electron metal electrodes and immersed in a solvent which intensely exchanges energy with that of traveling electrons. Charge and heat transfer kinetics was described by Marcus electron transfer theory.

Within the chosen model for the bridge, there exist two channels for the electron transport. As the bias voltage increases, these transport channels open up either simultaneously or successively depending on the character of the coupling between the bridge states on the electrodes, bias voltage distribution and the relationship between reorganization energies associated with the relevant molecular

states. Under certain conditions, a traveling electron can be temporarily trapped on the molecule thus blocking the corresponding channel. Then the channels open up successively which may result in NDR [27]. Here, we show that the same mechanism is responsible for qualitative changes in the behavior of heat currents. Features similar to NDR may appear in the behavior of steady state heat currents flowing to the electrodes and to the solvent. These features disappear when both transport channels are simultaneously accessible.

Also, we analyzed the heat currents and power produced by slow moving electron levels across a gate potential. Accounting for the total molecular energy rate and its heat, work and chemical components computed up to the terms linear in $\dot{\epsilon}_a$ ($\alpha=\{a,c\}$), it was established that the energy conservation was satisfied in the considered system in the case of a quasistatic driving. Separate studies of the total molecular energy rate components behavior show that the chemical work and heat coming from the electrodes and from the solvent take a significant part in \dot{E}_m when the driven level crosses the boundaries of the conduction window determined by the bias voltage. Otherwise, these contributions remain negligible and \dot{E}_m is determined by the reversible power generated in the system. We believe that the present results may be useful for better understanding of energy conversion and heat transfer in nanoscale systems.

CRediT authorship contribution statement

Natalya A. Zimbovskaya: Writing – review & editing, Writing – original draft, Validation, Methodology, Investigation, Conceptualization.

Declaration of competing interest

Authors declare that they have no competing financial interests or personal relationships which could influence the work reported in this paper.

Data availability

No data was used for the research described in the article.

Acknowledgments

The present work was supported by the U.S National Science Foundation (DMR-PREM 2122102).

References

- [1] A. Aviram, M.A. Ratner, Chem. Phys. Lett. 29 (1974) 277.
- [2] A. Nitzan, M.A. Ratner, Science 300 (2003) 1384.
- [3] J. Coropceanu, D.A. Cornil, F. da Silva, Y. Olivier, R. Silbey, J.-L. Brédas, Chem. Rev. 107 (2007) 926.
- [4] J.-C. Cuevas, E. Sheer, Molecular Electronics: An Introduction To Theory and Experiment, World Scientific, Singapur, 2010.
- [5] N.A. Zimbovskaya, M.R. Pederson, Phys. Rep 81 (2011) 1.
- [6] J. Ren, J.-X. Zhu, J.E. Gubernatis, C. Wang, B. Li, Phys. Rev. B 85 (2012) 155443.
- [7] T. Koch, J. Loos, H. Feshke, Phys. Rev. B 89 (2014) 155133.
- [8] N.A. Zimbovskaya, J. Phys.: Condens. Matter 26 (2014) 275303.
- [9] X. Li, J. Hinath, F. Chen, T. Masuda, N.G. Zhang, J. Tao, J. Am. Chem. Soc. 129 (2007) 11535.
- [10] C. Li, A. Mischenko, Z. Li, I.V. Pobelov, Th Wandlovski, X.-Q. Li, F. Wurthner, A. Bagrets, F. Evers, J. Phys.: Condens. Matter 20 (2008) 374122.
- [11] Z. Li, Y. Liu, S.F.L. Martens, I.V. Pobelov, Th Wandlovski, J. Am. Chem. Soc. 132 (2010) 8187.
- [12] R.A. Marcus, J. Chem. Phys. 24 (1956) 966.
- [13] R.A. Marcus, J. Chem. Phys. 24 (1956) 979.
- [14] R.A. Marcus, Rev. Modern Phys. 65 (1993) 599.
- [15] G.T. Craven, A. Nitzan, Proc. Natl. Acad. Sci. USA 113 (2016) 9421.
- [16] G.T. Craven, A. Nitzan, J. Chem. Phys. 146 (2017) 092305.
- [17] J.K. Sowa, J.A. Mol, G. Andrew, D. Briggs, E.M. Gauger, J. Chem. Phys. 149 (2018) 154112.
- [18] J.K. Sowa, J.A. Mol, E.M. Gauger, J. Phys. Chem. C 123 (2019) 4103.
- [19] H. Kirchberg, M. Thorwart, A. Nitzan, J. Phys. Chem. Lett. 11 (2020) 1729.
- [20] H. Kirchberg, A. Nitzan, J. Chem. Phys. 156 (2022) 094306.
- [21] A. Migliore, A. Nitzan, J. Am. Chem. Soc. 135 (2013) 9420.
- [22] A. Migliore, P. Schiff, A. Nitzan, Phys. Chem. Chem. Phys. 14 (2012) 13746.
- [23] A.M. Kuznetsov, I.G. Medvedev, Phys. Rev. B. 78 (2008) 153403.
- [24] A.M. Kuznetsov, I.G. Medvedev, J. Ulstrup, J. Chem. Phys. 131 (2009) 164703.
- [25] L. Yuan, L. Wang, A.R. Carriquez, L. Jiang, H.V. Annadata, M.A. Antonana, E. Barko, C.A. Nijhuis, Nat. Nanotechnol. 13 (2018) 322.
- [26] P.R. Bueno, T.A. Benites, J.J. Davis, Sci. Rep. 6 (2016) 18400.
- [27] A. Migliore, A. Nitzan, ACS Nano 5 (2011) 6669.
- [28] A.M. Kuznetsov, J. Ulstrup, J. Chem. Phys 116 (2002) 2149.
- [29] S. Corni, J. Phys. Chem. B 109 (2005) 3423.
- [30] V. Ben-Moshe, A. Nitzan, S. Skourtis, D.N. Beratan, J. Phys. Chem. C 114 (2010)
- [31] B. Muralidharan, S. Datta, Phys. Rev. B 76 (2007) 035432.
- [32] N.A. Zimbovskaya, A. Nitzan, J. Phys. Chem. B 124 (2020) 2632.
- [33] J.T. LÜ, J.-Sh. Wang, Phys. Rev. B 76 (2007) 165418.
- [34] T. Markussen, A.-P. Jauho, M. Brandbyge, Phys. Rev. B 79 (2009) 035415.
- [35] R. Härtle, M. Thoss, Phys. Rev. B 83 (2011) 125419.
- [36] R. Härtle, M. Thoss, Phys. Rev. B 83 (2011) 115414.
- [37] M. Kilguir, D. Segal, Phys. Rev. E 98 (2018) 012117.
- [38] A. Bruch, M. Thomas, S.V. Kusminskiy, F. von Oppen, A. Nitzan, Phys. Rev. B. 93 (2016) 115318.
- [39] Ludovico M.F., L. Arrachea, M. Moskalets, D. Sánchez, Phys. Rev. B 97 (2018) 041416.
- [40] Haughian P., M. Esposito, T.L. Schmidt, Phys. Rev. B 97 (2018) 085435.